AIP | Journal of Applied Physics

Crystallization properties and their drift dependence in phase-change memory studied with a micro-thermal stage

Chiyui Ahn, Byoungil Lee, Rakesh G. D. Jeyasingh, Mehdi Asheghi, G. A. M. Hurkx et al.

Citation: J. Appl. Phys. **110**, 114520 (2011); doi: 10.1063/1.3667295
View online: http://dx.doi.org/10.1063/1.3667295
View Table of Contents: http://jap.aip.org/resource/1/JAPIAU/v110/i11
Published by the American Institute of Physics.

Crystallization properties and their drift dependence in phase-change memory studied with a micro-thermal stage

Chiyui Ahn,[1,a)] Byoungil Lee,[1] Rakesh G. D. Jeyasingh,[1] Mehdi Asheghi,[2] G. A. M. Hurkx,[3] Kenneth E. Goodson,[2] and H.-S. Philip Wong[1]
[1]*Department of Electrical Engineering, Stanford University, Stanford, California 94305, USA*
[2]*Department of Mechanical Engineering, Stanford University, Stanford, California 94305, USA*
[3]*NXP-TSMC Research Center, Kapeldreef 75, 3001 Leuven, Belgium*

(Received 18 April 2011; accepted 14 November 2011; published online 12 December 2011)

The crystallization properties of phase-change memory (PCM) cells are studied at microsecond time scales using a novel micro-thermal stage. The time for recrystallization due to thermal disturbances is measured for varying amorphous volume fractions and annealing temperatures. PCM cells of intermediate resistances programmed with three different programming schemes are investigated and compared. For multi-bit programming, controlling the pulse-tail duration may be preferable as it has better retention characteristics than pulse-amplitude modulation or current-filament control. The effect of incomplete crystalline filaments on crystallization speed is experimentally investigated in this work, and the Arrhenius parameters are extracted from our crystallization time measurements to support a proposed unified mechanism for crystallization and drift. We have also found that recrystallization can be suppressed by more than 20% when there is a second of delay time between thermal disturbances. © *2011 American Institute of Physics*. [doi:10.1063/1.3667295]

I. INTRODUCTION

Phase-change memory (PCM) is a promising candidate for non-volatile memory technology.[1–3] Despite the demonstration of high speed, endurance, and scalability, a number of physical phenomena including crystallization and threshold switching are still not very well understood. Understanding these phenomena is critical in order to scale the devices for future technologies and to build a large array of reliable devices. One of the major challenges has been to study the crystallization property of the phase change memory cell due to inadequate understanding of crystallization physics, its strong dependence on materials and device geometry, and even the statistical nature of the crystallization process.[4] In particular, the recrystallization process—where a portion of the amorphous region formed by the reset process goes back to the crystalline phase, allowing current flow through the device and, hence, resulting in a low-resistance state—is highly dependent on the ambient temperature of the cell. This can be a serious issue when the temperature disturbance from the neighboring cells that are being programmed causes partial crystallization of the cell, resulting in retention failure.[5] In this work, the crystallization properties of the lateral PCM cell are investigated by ruling out possible dependence on materials, device geometries, or statistical variations by repetitively measuring a PCM cell in a fixed geometry.

It has been reported that the nature of the amorphous region and the availability of the nucleation/growth sites within the cell also strongly affect the crystallization process.[6] A study on how the time for crystallization due to thermal disturbance depends on the cell resistance or the amorphous fraction would, thus, help in developing more accurate crystallization models for the PCM cell. Another issue that is not well understood but is of practical importance in the development of multi-level PCM cells is the drift of the cell resistance. Recently, Ielmini *et al.*[7] proposed that a common physical interpretation for drift and crystallization is possible, based on a thermal excitation model for structural relaxation. Because the drift involves the increase in the amorphous state resistance with time and crystallization results in the decrease of amorphous state resistance with time, the dependence of one on the other is an important property to be investigated.

In this paper, we have developed an experimental methodology to investigate both the cell resistance and the drift dependences of the crystallization properties at shorter time scales (μs) using an on-chip micro-thermal stage (MTS). In order to allow the cell resistance to drift without thermal disturbances and thus separate drift from crystallization, we applied multiple short pulses to the MTS heater instead of monitoring the resistance change while being heated by a single long pulse as in Ref. 5. Our results using a doped SbTe alloy as phase-change material[8] show that the crystallization properties vary significantly with the nature of the amorphous region and depend on the drift properties of the cell as well.

II. MICRO-THERMAL STAGE AND PROGRAMMING SETUP

The crystallization time must be studied at a short time scale that is comparable to those involved in the device operation. In conventional measurement setups involving a hot chuck, the thermal time constant is too large to enable these studies. Hence, we use a structure called a micro-thermal stage that has a platinum (Pt) heater built on top of the lateral PCM cell (See Fig. 1), which is fabricated as reported in

a)Author to whom correspondence should be addressed. Electronic mail: cyahn@stanford.edu.

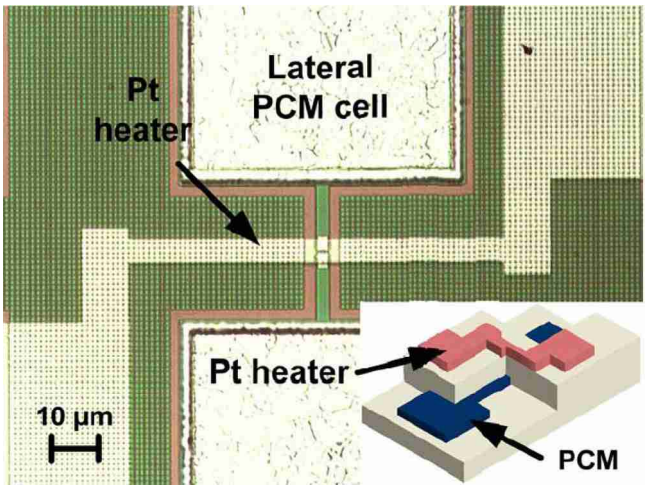

FIG. 1. (Color online) Top view microscope image of a lateral PCM cell with a micro-thermal stage (MTS) heater, which has been patterned with e-beam lithography techniques. The active PCM cell area where the PCM device and its local MTS heater intersect is about 140×400 nm^2. The inset shows the 3 D bird's eye view, and the SiO_x/SiN passivation layer with thickness of about 1 μm is used between the PCM cell and the Pt heater.

Ref. 9. The details of the structure and the principles of operation are already described in Ref. 5. The active PCM cell area is about 140×400 nm^2, with thickness of about 20 nm. The SiO_x/SiN layer was used for passivation (between the PCM cell and the Pt heater), with thickness of about 1 μm. This micro heater gives us the ability to control the temperature of the phase-change material in the microsecond time scale. The temperature is varied by changing the voltage amplitude of the heating pulse (V_{Pt}). The MTS temperature is calibrated by the temperature dependence of the resistivity of the Pt heater (ρ_{Pt}), using

$$\rho_{Pt} = \rho_0 + TCR_{Pt}(T_{HC} + R_H P) \quad (1)$$

where TCR_{Pt}, T_{HC}, P, and R_H are temperature coefficient of resistance of Pt, temperature of hot chuck on which the sample is placed, power delivered to the Pt heater, and thermal resistance between the Pt heater and the chuck, respectively. R_H of 1.06 °C/mW (Ref. 5) is used to extract the temperature rise from the delivered power to the MTS heater in this work.

The measurement setup consists of two sets of electrical pulses applied to the device, as shown in Fig. 2. One is the voltage pulse applied directly to the PCM cell to reset-program the PCM cell initially and read the cell resistance afterwards during heating. The reset pulse, which has a width of 50–100 ns and a rise/fall time of 2 ns is applied by a pulse pattern generator, Agilent 81110 A. Another pulse is the 100 μs-long heating pulse applied to the platinum heater (MTS). After applying the reset pulse and consequently programming the device to its high-resistance state, the heating pulse is applied to slowly recrystallize the cell. The heating pulse is applied as multiple short pulses or thermal disturbances separated by the time interval, t_p that can be controlled. During the application of the heating pulse, the Joule heating in the PCM device is neglected because of the small read current. It is found that the crystallization time is independent of the heating pulse duration (if we apply a longer pulse, then the number of heating pulses required to fully crystallize the PCM cell is reduced accordingly, making the total crystallization time unchanged), which implies that the applied multiple pulses can be considered as additive thermal disturbances in this work.

III. EXPERIMENTAL RESULTS AND DISCUSSION

Figure 3 shows the typical crystallization characteristic for a PCM cell with its own local MTS heater at the annealing temperature (T_A) of about 270 °C. With the heating pulse of 100 μs width and 1 μs rising/falling time turned on, the resistance gradually decreases until the crystallization path begins to be formed. After the cell is crystallized to a low-resistance state by the MTS heater, we observe that the resistance is larger by 15% to 30% than the set-programmed value by the electrical pulse. As can be seen in the inset of Fig. 3, the PCM cell is electrically programmed with reset/set resistance ratio of ~1000 and at least 100 cycles of set and reset programming are performed before each measurement of the crystallization time (t_{crys}) to verify that the PCM cell characteristics are stable at both set and reset resistance

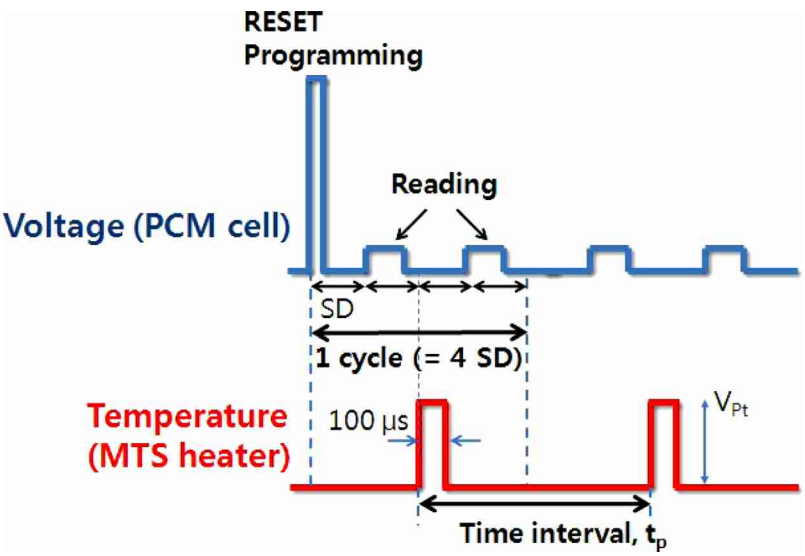

FIG. 2. (Color online) Electrical pulse profile for reset-programming, reading, and MTS heating. SD is a switch delay fixed at SD = 500 (ms) unless otherwise mentioned. Reading voltage is set at $V_{READ} \sim 0.1$ V to prevent the PCM cell from being recrystallized due to Joule heating. The 100 μs-long heating pulse is applied to the Pt heater with different voltage amplitudes, V_{Pt}, to give different annealing temperatures.

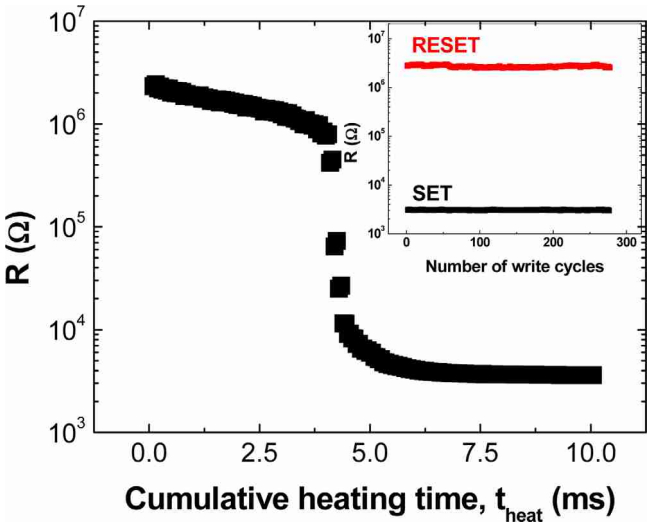

FIG. 3. (Color online) Crystallization by MTS heating (recrystallization due to thermal disturbances) at $T_A \sim 270$ °C. The crystallization time t_{crys} is extracted to be the cumulative heating time needed to form the first crystallization path within the amorphous region in the PCM cell. The inset shows the endurance characteristics with a high reset/set resistance ratio of ~ 1000.

values. By finding the number of annealing pulses required to fully crystallize the PCM cell in Fig. 3, the crystallization time is found to be about 4 ms (40×100 μs) for the annealing temperature of 270 °C with V_{Pt} of about 6 V. The precise value of the crystallization time may depend on how the crystallization time is determined (e.g., differentiation of the resistance versus time curve to find the point where the resistance begins to abruptly decrease during heating or finding the time required for the initial amorphous state to reach a resistance of several times the set one) from the given resistance (R) versus cumulative heating time (t_{heat}) characteristics. Nevertheless, our preliminary analysis shows that any employed method to calculate the crystallization time makes little difference in the overall conclusion once the method is applied consistently for t_{crys} determination.

To see the dependence of the crystallization time on the initial cell resistance, the PCM cells were programmed to resistances of 2, 3, 4, and 5 M Ω and the crystallization times were measured for various temperatures. The result is shown in Fig. 4(a). As seen in the figure, the crystallization time exponentially falls off with increasing temperature following the Arrhenius equation,[10] from ~ 50 ms to ~ 200 μs for temperatures ranging from ~ 230 °C to ~ 290 °C when the initial cell resistance is set at ~ 3 M Ω by adjusting the reset voltage. To study the crystallization for different cell resistances, a 100 ns-long voltage pulse with rising and falling time of 2 ns was applied to the cell in the set state with its amplitude increased in a few steps of mV to achieve different cell resistances. If we start the MTS heating with the higher cell resistances of 4 M and 5 M Ω, the crystallization time increases implying that the increased amorphous fraction makes the crystallization process harder. The activation energy for crystallization[11] is extracted from the slope of the t_{crys} versus $1/kT_A$ (k is the Boltzmann constant) plot in Fig. 4(a), and it is found to be about 2 eV, which agrees well with the reported value in our previous work.[5] It should be noted that

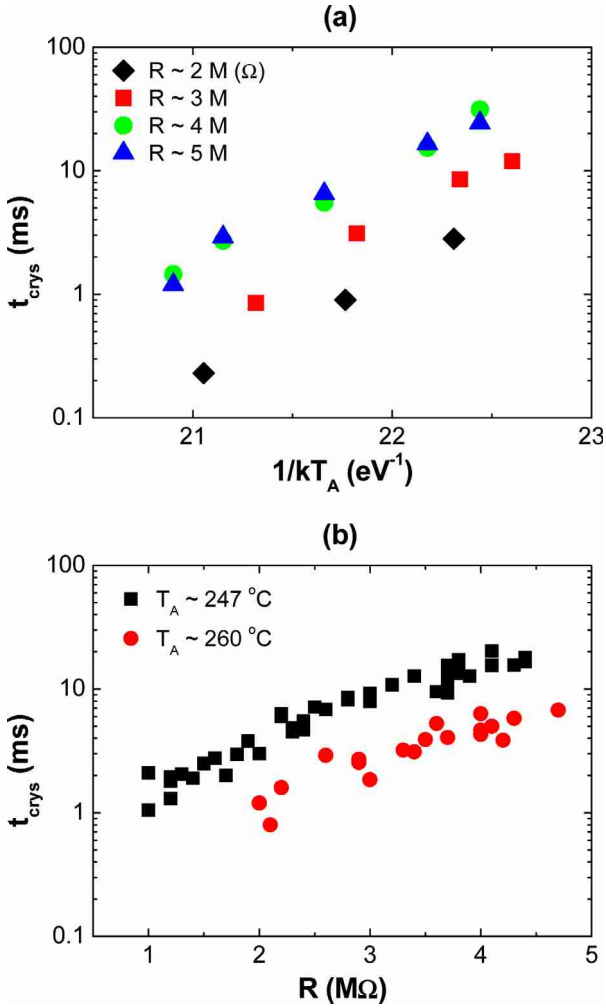

FIG. 4. (Color online) (a) Temperature (T_A) dependence of the crystallization behavior for different cell resistances and (b) cell resistance (R) dependence for two different temperatures. PCM cells are initially programmed to different resistances by the reset pulse of different voltage amplitudes.

further increase of the cell resistance toward the full-reset value of about 6 M Ω results in almost the same crystallization time. This trend of an initial increase of crystallization time with increasing cell resistance and saturation afterward is more clearly observed in Fig. 4(b), which shows the crystallization times as a function of cell resistances, R. The recrystallization time due to thermal disturbances is found to saturate as the cell resistance increases, and it may be attributed to the fact that the amorphous volume of the lateral PCM cell does not change so much once it reaches near the full-reset state.

We next investigate the difference in the crystallization behavior for three different programming schemes used in multi-level applications. In the first scheme, the various intermediate resistances are obtained by applying the reset pulses of different amplitudes (pulse-amplitude control, PAC). In the second scheme, a reset pulse with a maximum reset amplitude is applied to the cell and the fall time of this pulse is controlled to vary the quenching time of the molten phase-change material within the cell (pulse-tail duration control, PDC).[12] The longer the fall-time, the smaller the

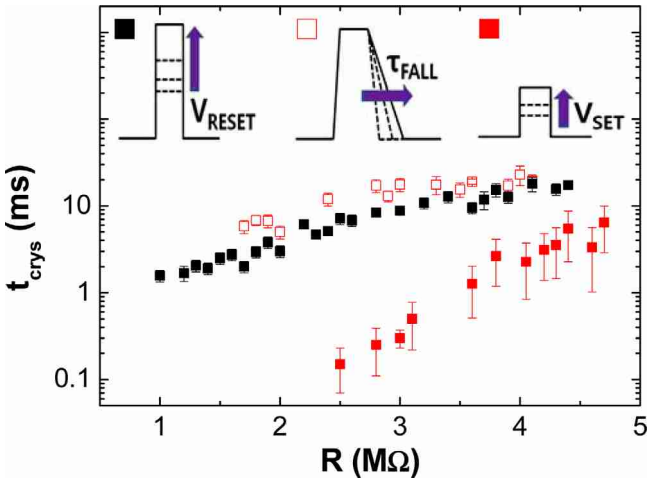

FIG. 5. (Color online) Crystallization times for the PCM cells in the intermediate states by different programming schemes. Programming scheme 1 (black solid square) is to control the pulse-amplitude (V_{RESET}) starting from the full-set state, scheme 2 (empty red square) modulates the pulse-tail duration (τ_{FALL}) starting from the full-reset state, and scheme 3 (solid red square) represents the current-filament control by changing the voltage amplitude of the set pulse starting from the full-reset state. T_A is maintained at 247 °C.

resistance as the molten material will have sufficient time to crystallize during the quenching process. In the last scheme, we control the filament formation during the set process[13] by applying set pulses of varying amplitudes (current-filament control, CFC) to the cell which is initially programmed to the full-reset state. For each intermediate resistance state, the cell is subjected to consecutive thermal disturbance pulses causing a temperature rise of about 220 °C. The crystallization times for the different intermediate states, achieved by different programming schemes, are shown in Fig. 5. It can be seen that for the cells with the same resistance state, the crystallization time is much smaller for the current filament control case than the other schemes. This can be explained by a growth-dominated mechanism of the crystallization starting from the already-present crystalline filament boundaries in these intermediate states.[13] For the other two schemes, the crystallization can start only from the outer boundaries of the amorphous region.

Figure 6 illustrates how the growth-dominated crystallization process occurs differently for three different programming schemes of pulse-amplitude control, pulse-tail duration control, and current-filament control. It should be noted from Fig. 6 that crystallization due to thermal disturbances (MTS heating) can occur at the incomplete crystalline filament as well as at the outer crystalline/amorphous boundary only for the current-filament control case. The other two cases have less possibility to form crystalline nuclei inside of the amorphous region because their intermediate state formation starts from a completely molten volume due to high voltage pulse applied. The pulse-tail duration scheme starting from the full-reset state (the cell in this intermediate state is called "partial set" state because it is being partially set-programed) and the pulse-amplitude control scheme starting from the full-set state (the cell is in the partial reset state) thus show slower recrystallization or better retention due to the more uniform nature of the amorphous region formed within the cell and the lack of any random crystallites or crystal filaments in the bulk amorphous region as well.

Because our crystallization time measurements show typical Arrhenius behavior, it is possible to extract the two Arrhenius parameters of activation energy E_A and pre-exponential factor τ_0 of the Meyer-Neldel (MN) model.[14] The MN rule predicts that τ_0 is given by,

$$\tau_0 = \tau_{00} \exp(-E_A/kT_{MN}), \tag{2}$$

to compensate for the structural relaxation process with a high activation energy barrier. The energy Δ (= kT_{MN}) in Eq. (2) is of particular importance to understand the structural relaxation (SR) process as it represents the amount of thermal excitation energy that should be provided by a single electron-phonon interaction[15] to overcome the activation barrier E_A. E_A is experimentally determined by measuring the crystallization times of the PCM cell in the partial reset state for two different temperatures and then τ_0 is easily obtained by plugging the obtained E_A value into the Arrhenius equation for a given temperature T,

$$t_{crys} = \tau_0 \exp(E_A/kT). \tag{3}$$

We find in this work that E_A and τ_0 are about 2.15 eV and 4.45×10^{-24} s, respectively, with no dependence of these parameters on the amorphous cell resistances. The parameters of E_A and τ_0 have been obtained in previous research by solely measuring the resistance drift[7] or the crystallization

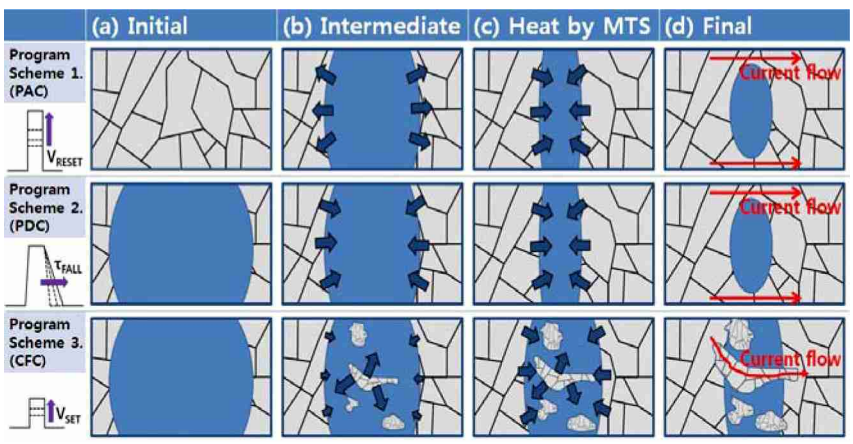

FIG. 6. (Color online) Crystallization processes of a lateral PCM cell from (a) initial state through (b) intermediate state formed by different partial programming schemes of PAC (pulse-amplitude control), PDC (pulse-tail duration control), and CFC (current-filament control); and (c) cell state heated uniformly by the MTS to (d) final (set) state. The arrows in (b) represent the amorphous or crystalline growth when the voltage amplitude or the fall time of the reset pulse is increased in the PAC or PDC scheme, respectively, and the crystallization occurring both at outer boundaries and at filaments is depicted in the CFC scheme.

time.[16,17] Because our experimental setup allows the crystallization process to be affected by the resistance drift, comparing the Arrhenius parameters in this work with those in the literature would be valuable to understand the crystallization process within the framework of the SR model. Our measured Arrhenius parameters align well with a fit line in the τ_0 versus E_A plot in Ref. 7 and it suggests that crystallization and resistance drift can be explained by the Meyer-Neldel equation with the same physical parameters of τ_{00} and T_{MN}. The proposed unified mechanism of structural relaxation for crystallization and drift[7] is confirmed here. Our experimental results also support the idea in Ref. 7 that the extremely small pre-exponential value for crystallization (on the order of 10^{-24} s) is attributed to the large activation energy barrier.

Lastly, we investigate the dependence of the crystallization time on the resistance drift in Fig. 7 with the PCM cells programmed to the same initial amorphous resistances. The effect of drift is incorporated by changing the time interval (t_p) between the consecutive heating pulses applied during the crystallization process. This difference in time intervals between the two pulses will cause the cells to drift differently, as the resistance drift is related to time by a power-law equation.[18] Hence, any change in the crystallization time (i.e., cumulative heating time to achieve full crystallization) between the different cases of time interval should be directly due to the additional drift occurring in the cell states. It is clearly seen in Fig. 7 that the crystallization occurs faster as we decrease the time interval from 10 s to 1.2 s. To understand the observed dependence of crystallization on drift, it should be noted that the annealed cells are not disturbed by the same number of MTS pulses. If they have been stressed by the same number of MTS pulses, then the cells that had larger time intervals between the heating pulses would not have reached complete crystallization compared to those that had shorter intervals during the thermal disturbance. Hence, with the same number of MTS pulses, it is not possible to compare the crystallization time for larger time intervals with that for smaller intervals. Because the on parts of the MTS pulse are exactly the same for both cases, the difference in the number of MTS pulses and, thus, in crystallization time should come from the off parts of the MTS pulse, which are modulated by different t_p values. Even though the temperature in the off parts of the MTS pulse is just room temperature, a few seconds of long wait time for the cell to drift should lead to a significant amount of resistance drift. At high temperatures (during the on part of MTS pulses), the resistance drift is not accelerated linearly with temperature, possibly due to the simultaneous crystallization process,[5] and the notable difference in t_{crys} for different t_p values should come from the different amount of resistance drift during the off part. Figure 7 also shows that the statistical variation that arises from the random nature of the crystallization process is found to be quite large, so more than 10 samples of crystallization time measurements have been averaged for each time interval to give statistically reasonable values with 1-sigma (σ) uncertainties. The linear fit line in the log-scaled t_{crys} versus t_p plot lies within the statistical error bars, and thus we conclude that the measured crystallization time in Fig. 7 depends exponentially on the time interval between the multiple pulses. Because the drift of the reset resistance follows the phenomenological power law with time, it is concluded from the above results that the resistance drift can decelerate the crystallization process. Our preliminary analysis shows that the increased crystallization time with additional resistance drift is attributed to the increased effective activation energy. This is because the different amount of resistance drift, which is expected to have a smaller activation barrier than the crystallization process has,[7] should give different "effective" E_A values when the crystallization time is measured with varying t_p values. A separate and detailed study on the physical basis of what we observed in Fig. 7 is being carried out currently and the results will be published elsewhere. It is noted from this finding that if a PCM cell is reset-programmed, it would be better to program the neighboring cells at a later time, allowing the current cell to drift for some time. This would lower the probability of cell failure due to thermal disturbances.

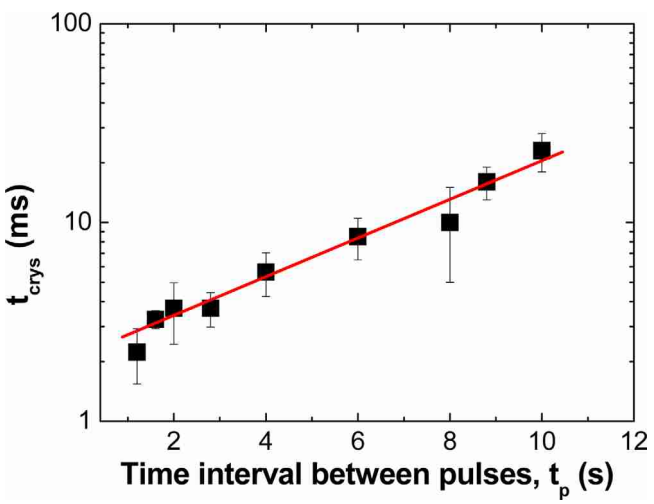

FIG. 7. (Color online) The crystallization time (t_{crys}) vs time interval between pulses (t_p). The error bar shows the statistical variations (1σ) from repetitive measurements of the crystallization time, and the linear fit line is drawn to show that it lies within the uncertainties. The annealing temperature is set at $T_A \sim 255$ °C.

IV. SUMMARY AND CONCLUSION

In this work, we have used a micro-thermal stage to study the crystallization behavior of lateral PCM cells in the microsecond time scale, and the dependence of the crystallization time on the cell resistance and the temperature has been investigated. The crystallization behavior for the intermediate states obtained by various programming schemes were compared, and it was found that the pulse-tail duration control has the best retention characteristics due to the uniform nature of the amorphous region formed. Furthermore, the effect of the resistance drift on the crystallization time was studied, showing that a longer drift process leads to better retention. This also suggests a better programming scheme to reduce failure in the memory bits due to thermal disturbances from the neighboring cells. This study on the crystallization process of

a PCM cell leads to better understanding of physical origins of crystallization within a PCM cell.

ACKNOWLEDGMENTS

The authors would like to thank Dr. SangBum Kim of the IBM T. J. Watson Research Center for technical discussions. This work is supported in part by NXP through the Stanford Center for Integrated Systems (CIS) custom research program, the National Science Foundation (NSF) through grant CBET-0853350, and the MSD Focus Center, one of the six research centers funded under the Focus Center Research Program (FCRP), a Semiconductor Research Corporation entity.

[1]S. Lai, IEEE International Electron Devices Meeting (Washington, DC, Dec. 8–10, 2003), p. 255.
[2]Y. C. Chen, C. T. Rettner, S. Raoux, G. W. Burr, S. H. Chen, R. M. Shelby, M. Salinga, W. P. Risk, T. D. Happ, G. M. McClelland, M. Breitwisch, A. Schrott, J. B. Philipp, M. H. Lee, R. Cheek, T. Nirschl, M. Lamorey, C. F. Chen, E. Joseph, S. Zaidi, B. Yee, H. L. Lung, R. Bergmann, and C. Lam, IEEE International Electron Devices Meeting IEEE, International Electron Devices Meeting (San Francisco, CA, Dec. 11–13, 2006), p. 346910.
[3]M. Breitwisch, T. Nirschl, C. F. Chen, Y. Zhu, M. H. Lee, M. Lamorey, G. W. Burr, E. Joseph, A. Schrott, J. B. Philipp, R. Cheek, T. D. Happ, S. H. Chen, S. Zaidr, P. Flaitz, J. Bruley, R. Dasaka, B. Rajendran, S. Rossnage, M. Yang, Y. C. Chen, R. Bergmann, H. L. Lung, and C. Lam, IEEE Symposium on VLSI Technology (Kyoto, Japan, June 12–16, 2007), p. 100.
[4]U. Russo, D. Ielmini, A. Redaelli, and A. L. Lacaita, IEEE Trans. Electron Devices **53**, 3032 (2006).
[5]S. Kim, B. Lee, M. Asheghi, G. A. M. Hurkx, J. Reifenberg, K. Goodson, and H.-S. P. Wong, IEEE Trans. Electron Devices **58**, 584 (2011).
[6]S. Meister., "In-Situ TEM Study of Nanoscale Phase Change Memory Cells" Ph.D. dissertation (Stanford University, 2010).
[7]D. Ielmini, M. Boniardi, A. L. Lacaita, A. Redaelli, and A. Pirovano, Microelectron. Eng. **86**, 1942 (2009).
[8]M. H. R. Lankhorst, W. S. M. M. Ketelaars, and R. A. M. Wolters, Nature Mater. **4**, 347 (2005).
[9]D. Tio Castro, L. Goux, G. A. M. Hurkx, K. Attenborough, R. Delhougne, J. Lisoni, F. J. Jedema, M. A. A. in't Zandt, R. A. M. Wolters, D. J. Gravesteijn, M. A. Verheijen, M. Kaiser, R. G. R. Weemaes, and D. J. Wouters, IEEE International Electron Devices Meeting (Washington, DC, Dec. 10–12, 2007), p. 315.
[10]A. Redaelli, A. Pirovano, A. Benvenuti, and A. L. Lacaita, J. Appl. Phys. **103**, 111101 (2008).
[11]G. Ruitenberg, A. K. Petford-Long, and R. C. Doole, J. Appl. Phys. **92**, 3116 (2002).
[12]T. Nirschl, J. B. Phipp, T. D. Happ, G. W. Burr, B. Rajendran, M. H. Lee, A. Schrott, M. Yang, M. Breitwisch, C. F. Chen, E. Joseph, M. Lamorey, R. Cheek, S. H. Chen, S. Zaidi, S. Raoux, Y. C. Chen, Y. Zhu, R. Bergmann, H. L. Lung, and C. Lam, IEEE International Electron Devices Meeting (Washington, DC, Dec. 10–12, 2007), p. 461.
[13]D. Mantegazza, D. Ielmini, A. Pirovano, and A. L. Lacaita, IEEE Electron Device Lett. **31**, 341 (2010).
[14]W. Meyer and H. Neldel, Z. Tech. Phys. (Liepzig) **12**, 588 (1937).
[15]A. Yelon, B. Movaghar, and H. M. Branz, Phys. Rev. B **46**, 12244 (1992).
[16]A. Redaelli, D. Ielmini, U. Russo, and A. Lacaita, IEEE Trans. Electron Devices **53** 3040 (2006).
[17]A. Pirovano, A. Redaelli, F. Pellizzer, F. Ottogalli, M. Tosi, D. Ielmini, A.L. Lacaita, and R. Bez, IEEE Trans. Device Mater. Reliab. **4**, 422 (2004).
[18]D. Ielmini, S. Lavizzari, D. Sharma, and A. Lacaita, IEEE International Electron Devices Meeting (Washington, DC, Dec. 10–12, 2007), p. 939.